Supportive Information

S1 Structural Data

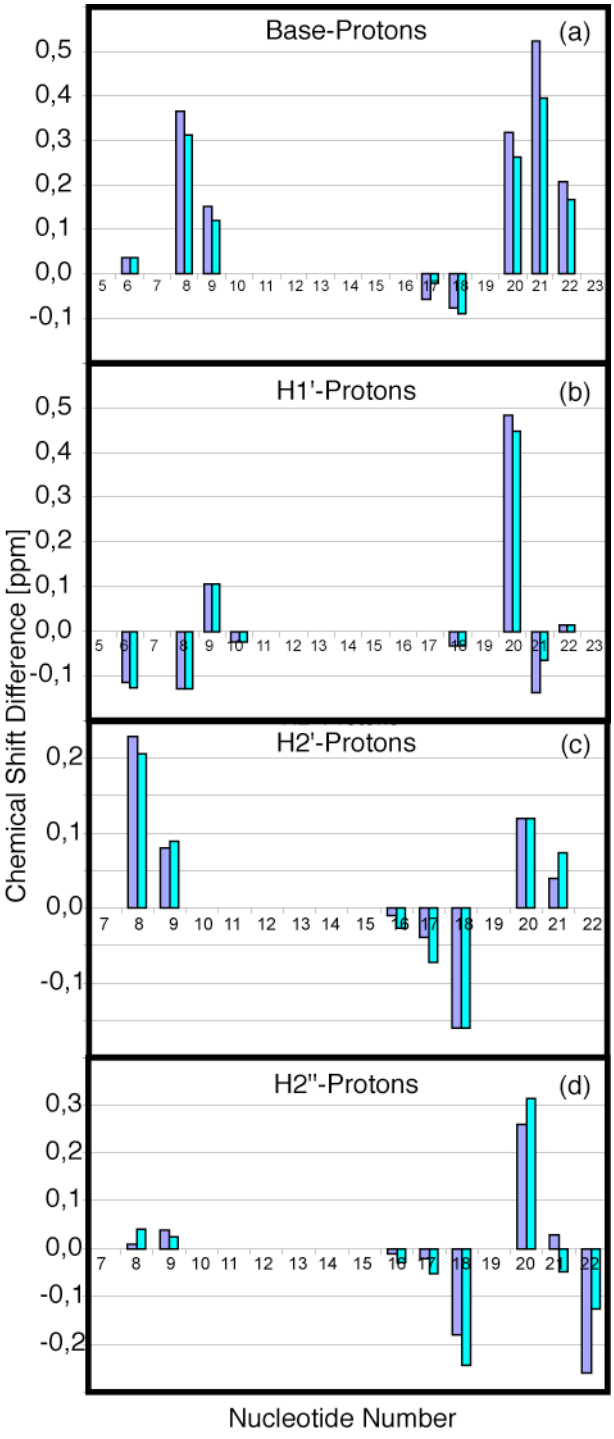

Figure S1.1 Experimental differences in chemical shifts of 5'-AAX and the corresponding unmodified strand 5'-AAT (turquoise), (a) representing protons of the bases, (b)-(d) representing sugar protons. Based on differences of the chemical shift of H6/H8 base protons of the duplexes 5'-AAX and

its reference 5'-AAT, we conclude that all nearest neighbor bases except A6 are significantly affected by the replacement of thymine by the acridinium X^+. Within the accuracy of the chemical shift information, we consider changes of the order of $\Delta\delta > 0.25$ ppm as significant and conclude that the structural perturbation depends on directionality. As depicted in Figure S1.1 the structural distortion of the environment of the acridinium is more pronounced in 3' direction than in 5' direction for both the X^+ modified strand and its counterstrand. (Figure S1.1). The agreement between experimental chemical shift differences and those calculated on the basis of the final 5'-AAX and 5'-AAT structures is excellent.

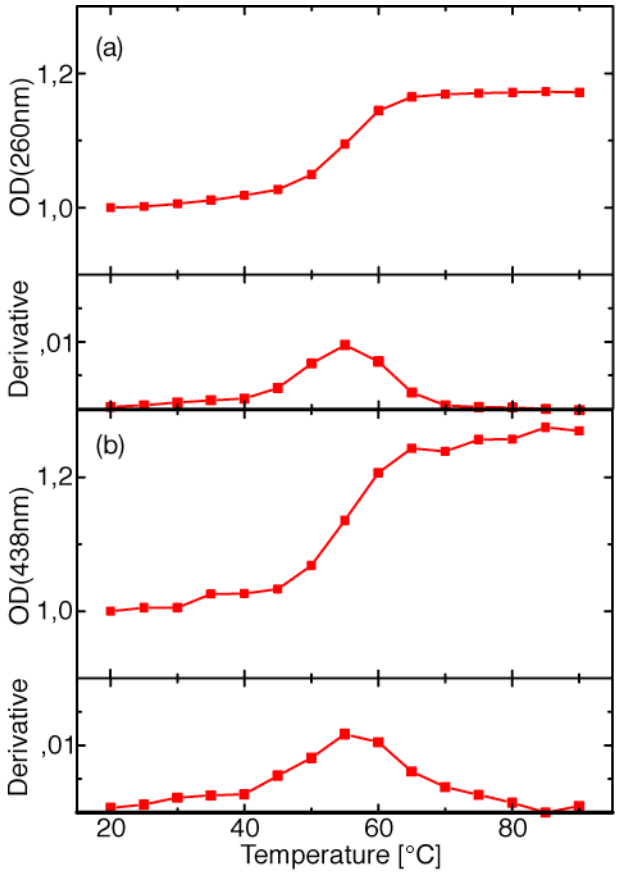

Figure S1.2 Melting curves of 5'-AAX measured in the absorption region of the nucleobases at 260 nm (a) and the acridinium X^+ at 438 nm(b).

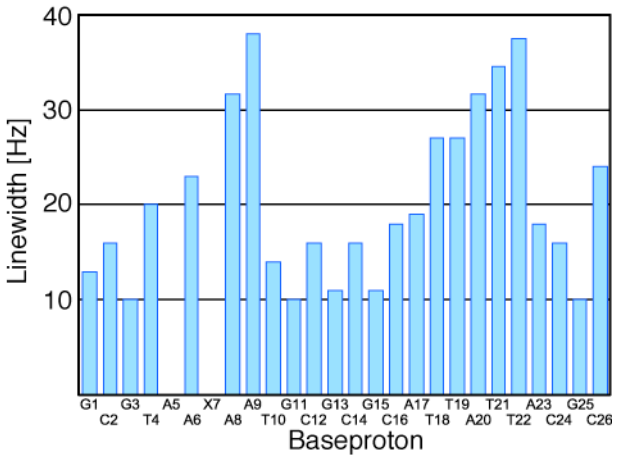

Figure S1.3 Linewidths of 5'-AAX base protons.

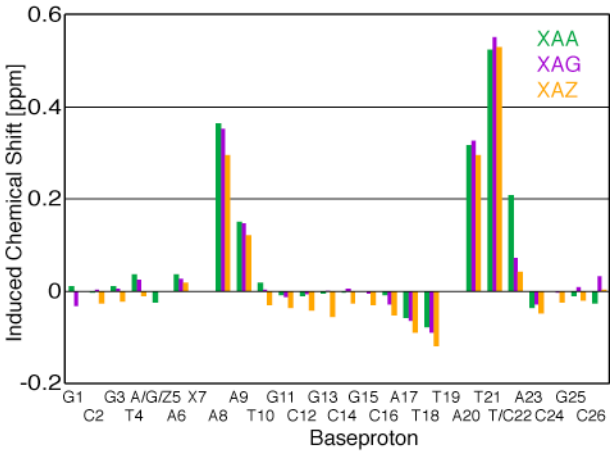

Figure S1.4 Induced chemical shifts of 5'-AAX, 5'-GAX and 5'-ZAX.

Nucleotide	H1' proton Reference	H1' proton Konf A	Base proton Reference	Base proton Konf A
G1	6,024	6,020	7,976	7,988
C2	5,798	5,810	7,440	7,438
G3	5,990	6,013	7,918	7,929
T4	5,640	5,720	7,185	7,223
A5	5,959	5,944	8,248	8,225
A6	6,121	6,006	8,126	8,163
T7	5,574	-	7,055	-
A8	5,970	5,840	8,173	8,538
A9	6,148	6,253	8,113	8,264
T10	5,736	5,711	7,010	7,030
G11	5,850	5,833	7,843	7,835
C12	5,827	5,919	7,357	7,348
G13	6,189	6,186	7,960	7,957
C14	5,818	5,817	7,647	7,646
G15	5,940	5,944	7,970	7,970
C16	5,666	5,651	7,395	7,387
A17	6,315	6,278	8,346	8,288
T18	5,921	5,888	7,183	7,107
T19	5,867	-	7,403	-
A20	6,257	6,741	8,308	8,626
T21	5,922	5,785	7,183	7,707
T22	5,755	5,796	7,355	7,563
A23	6,180	6,156	8,296	8,260
C24	5,609	5,612	7,265	7,265
G25	5,970	5,974	7,886	7,876
C26	6,222	6,211	7,486	7,460

Table S1.1 Chemical shift for 5'-AAX induced by X^+ modification.

Nucleotide	H1' proton Reference	H1' proton Konf A	Base proton Reference	Base proton Konf A
G1	6,028	6,043	7,982	7,950
C2	5,809	5,818	7,456	7,460
G3	6,023	6,033	7,938	7,944
T4	5,791	5,810	7,132	7,158
G5	5,626	-	7,884	-
A6	6,212	6,100	8,167	8,195
T7	5,618	-	7,116	-
A8	5,982	5,838	8,205	8,558
A9	6,168	6,258	8,136	8,283
T10	5,748	5,697	7,032	7,035
G11	5,865	5,838	7,852	7,840
C12	5,842	5,828	7,361	7,355
G13	6,198	6,184	7,966	7,967
C14	5,828	5,826	7,653	7,658
G15	5,955	5,944	7,982	7,978
C16	5,687	5,665	7,412	7,384
A17	6,328	6,274	8,354	8,290
T18	5,930	5,888	7,200	7,112
T19	5,862	-	7,412	-
A20	6,261	6,750	8,314	8,642
T21	5,905	-	7,162	7,714
C22	5,567	5,570	7,506	7,578
A23	6,196	6,171	8,289	8,262
C24	5,622	5,627	7,260	7,258
G25	5,979	5,986	7,886	7,896
C26	6,219	6,238	7,466	7,500

Table S1.2: Chemical shift for 5'-GAX induced by the X^+ modification.

Nucleotide	Base proton Reference	Base proton Konf A
G1	7,984	-
C2	7,454	7,428
G3	7,931	7,910
T4	7,141	7,132
G5	6,864	-
A6	8,112	8,131
T7	7,130	-
A8	8,207	8,503
A9	8,139	8,261
T10	7,036	7,006
G11	7,855	7,819
C12	7,363	7,321
G13	7,967	7,912
C14	7,656	7,630
G15	7,984	7,954
C16	7,414	7,363
A17	8,356	8,267
T18	7,198	7,079
T19	7,414	-
A20	8,308	8,603
T21	7,162	7,693
C22	7,484	7,527
A23	8,274	8,227
C24	7,255	7,231
G25	7,889	7,870
C26	7,477	7,481

Table S1.3 Chemical shift for 5'-ZAX induced by the X^+ modification. H1' is not assigned.

1st strand		C1'-C2'	C2'-C3'	Phase	Ampli	Pucker	C1'	C2'	C3'
1)GUA	1	34.72	-36.34	168.53	37.89	C2'-endo	106.0	101.7	102.7
2)CYT	2	35.05	-33.79	160.97	36.54	C2'-endo	105.8	101.9	103.4
3)GUA	3	36.75	-35.04	160.32	38.09	C2'-endo	105.7	101.7	103.0
4)THY	4	32.88	-31.20	159.53	34.04	C2'-endo	106.0	102.6	103.7
5)ADE	5	34.41	-34.03	163.47	36.32	C2'-endo	106.0	101.9	103.2
6)ADE	6	34.33	-29.66	151.71	34.56	C2'-endo	105.9	102.6	103.7
7)LIG	7								
8)ADE	8	34.89	-32.35	157.67	35.80	C2'-endo	105.9	102.2	103.5
9)ADE	9	31.21	-34.11	172.24	35.13	C2'-endo	106.3	102.4	103.0
10)THY	10	37.96	-30.75	146.17	38.00	C2'-endo	105.2	101.9	103.7
11)GUA	11	32.56	-37.17	176.09	38.02	C2'-endo	106.2	101.8	102.3
12)CYT	12	35.82	-35.94	164.62	38.09	C2'-endo	105.7	101.5	103.0
13)GUA	13	34.27	-38.62	175.16	39.61	C2'-endo	106.1	101.4	102.0

Torsions		Chi C1'-N	Gamma C5'-C4'	Delta C4'-C3'	Epsil C3'-O3'	Zeta O3'-P	Alpha P-O5'	Beta O5'-C5'
1)GUA	1	-95.23	58.95	147.61	173.45	-107.35	-47.94	-177.93
2)CYT	2	-109.69	38.11	142.35	-172.24	-135.70	-22.54	159.06
3)GUA	3	-101.28	31.15	143.56	174.36	-106.89	-46.86	176.19
4)THY	4	-111.64	47.94	139.57	45.78	83.37	-175.01	-153.43
5)ADE	5	-80.05	19.96	144.18	-85.99	171.07	-82.94	136.24
6)ADE	6	-95.21	35.99	136.09	67.45	-179.06	.....	.....
7)LIG	7	.....	.....	.....	.....	.....	.....	.....
8)ADE	8	-90.10	73.99	140.78	-171.43	-129.75	-47.19	178.84
9)ADE	9	-95.76	32.00	146.69	173.35	-108.65	-38.39	168.57
10)THY	10	-114.07	43.11	134.76	-177.38	-119.77	-29.99	-172.35
11)GUA	11	-99.91	19.95	150.63	171.69	-111.87	-40.29	176.45
12)CYT	12	-111.09	38.46	145.44	-176.68	-120.19	-37.91	-174.83
13)GUA	13	-97.77	32.41	152.48	.....	.....	.....	.....

2nd strand		C1'-C2'	C2'-C3'	Phase	Ampli	Pucker	C1'	C2'	C3'
1)CYT	26	35.73	-28.89	145.87	35.81	C2'-endo	105.5	102.3	104.1
2)GUA	25	31.96	-38.12	179.77	38.91	C2'-endo	106.3	101.6	102.1
3)CYT	24	40.93	-35.83	152.85	41.35	C2'-endo	104.9	100.6	103.1
4)ADE	23	29.60	-35.75	180.67	36.46	C3'-exo	106.5	102.2	102.6
5)THY	22	26.33	-36.39	190.77	37.76	C3'-exo	106.8	102.1	102.3
6)THY	21	13.43	-26.18	209.01	30.45	C3'-exo	107.2	104.4	103.5
7)ADE	20	-22.63	33.93	16.14	36.02	C3'-endo	107.3	102.7	102.4
8)THY	19	36.40	-31.80	152.36	36.79	C2'-endo	105.4	101.9	103.7
9)THY	18	33.09	-32.15	161.75	34.61	C2'-endo	106.0	102.4	103.6
10)ADE	17	21.96	-31.75	193.77	33.28	C3'-exo	107.0	103.5	102.9
11)CYT	16	39.21	-36.51	158.08	40.29	C2'-endo	105.1	101.0	102.8
12)GUA	15	34.55	-38.17	173.32	39.25	C2'-endo	106.0	101.4	102.2
13)CYT	14	32.36	-35.32	172.11	36.40	C2'-endo	106.2	102.0	102.9

Torsions		Chi C1'-N	Gamma C5'-C4'	Delta C4'-C3'	Epsil C3'-O3'	Zeta O3'-P	Alpha P-O5'	Beta O5'-C5'
1)CYT	26	-109.15	54.18	134.24	.....	.....	.....	.....
2)GUA	25	-92.52	-20.66	153.89	170.39	-95.30	-70.94	-173.55
3)CYT	24	-105.58	42.61	141.33	-76.08	136.35	-20.56	134.62
4)ADE	23	-88.93	-45.21	151.38	172.22	-104.57	-45.89	174.77
5)THY	22	-107.66	148.21	156.68	-170.19	-135.33	39.44	150.79
6)THY	21	-96.70	6.44	151.13	54.34	73.94	121.97	125.44
7)ADE	20	-81.37	109.49	86.03	58.60	-51.74	-98.79	-100.13
8)THY	19	-99.10	13.37	138.25	178.92	-110.16	-47.85	-109.40
9)THY	18	-105.97	33.32	142.49	-163.41	-106.08	-35.46	175.10
10)ADE	17	-100.60	29.87	152.36	-179.55	-116.73	-38.10	173.04
11)CYT	16	-114.35	49.38	142.64	168.39	-102.58	-54.18	-140.87
12)GUA	15	-98.46	28.53	150.66	170.09	-108.66	-45.86	171.87
13)CYT	14	-109.81	25.70	148.39	-174.88	-122.11	-34.69	-177.34

Table S1.4: |J| backbone parameters

S2 Femtosecond Kinetics

Femtosecond Time Resolved Difference Absorbance Spectra. The contribution of $X^{\bullet}$ radical absorption to difference absorbance can be estimated by comparing the difference absorbance spectra of 5'-AAX, where no radical is formed, and 5'-AZX with maximal radical pair formation on the sub-ps time scale. As shown in Figure S2.1, at wavelengths between 470 nm and 560 nm the *difference* between contributions from the excited state $^1(X^+)^*$ and $X^{\bullet}$ signal to the difference absorption signal is maximal. Since at 530 nm the difference absorption of 5'-AAX is negative, but small, additional radical absorption can invert the sign of the transient absorption signal.

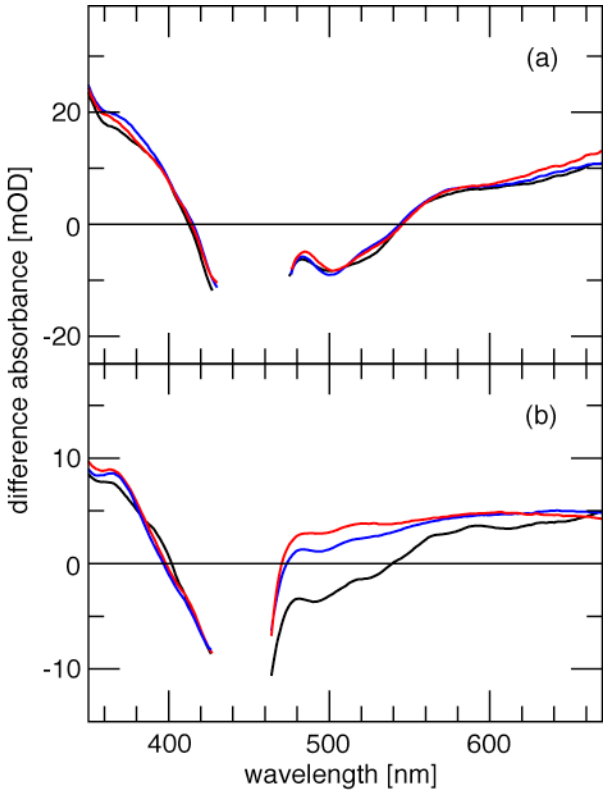

Figure S2.1 Difference absorbance spectra of 5'-AAX (a) and 5'-AZX (b) excited at 440 nm and probed after 100 fs (—), 2 ps (—), and 5 ps (—) at 273 K. While in 5'-AAX only $^1(X^+)^*$ is populated, in 5'-AZX a significant population of the radical pair leads to the development of a positive transient.[17]

Kinetic Behaviour of NMR Samples

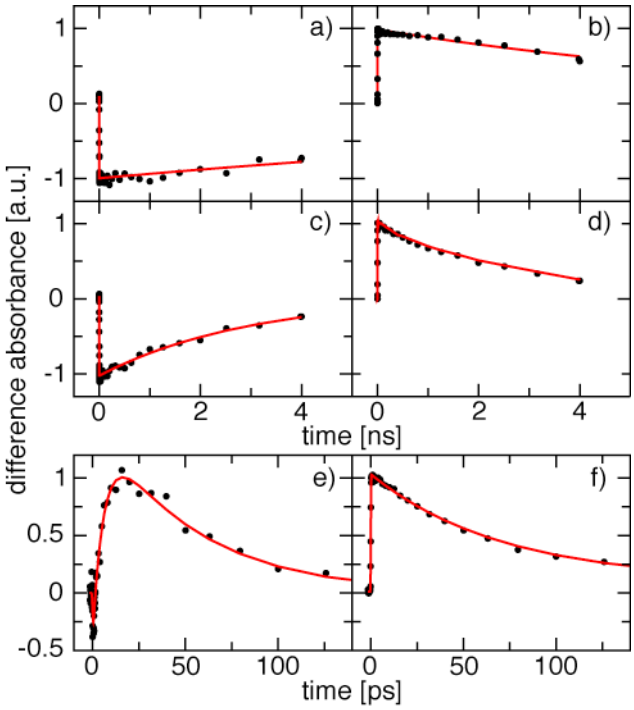

Figure S2.2 Temporal traces of difference absorbance of 5'-AAX (a, b), 5'-GAX (c, d) and 5'-ZAX (e, f) of NMR samples. Excitation at 455 nm. The time traces b, d, and f are probed at 650 nm showing absorption signals from $(X^{+})^{*}$ and $X^{\bullet}$. Time traces a and c are recorded at 500 nm and probe the stimulated emission from $(X^{+})^{*}$. The time trace e probed at 530 nm is indicative of a superposition of stimulated emission from the $(X^{+})^{*}$ (with a negative sign) and $X^{\bullet}$ radical absorption (with a positive sign). Sample temperatures were 295 K (a-d) and 273 K (e-f). Least square fits (solid lines) give for: 5'-AAX: > 10 ns for both traces (a-b), for 5'-GAX: 3 ns with ~ 30 % background absorption decaying at times > 10 ns for both traces (c-d), and for 5'-ZAX: 8.6 ps (positive sign) and 70 ps (negative sign) in traces (e), and 82 ps (f).